ELSEVIER

Earth and Planetary Science Letters 194 (2002) 343–358

EPSL

www.elsevier.com/locate/epsl

Changes in remanence, coercivity and domain state at low temperature in magnetite

Özden Özdemir [a,*], David J. Dunlop [a], Bruce M. Moskowitz [b]

[a] *Department of Physics, University of Toronto at Mississauga, Mississauga, ON, Canada L5L 1C6*
[b] *Institute for Rock Magnetism, University of Minnesota, Minneapolis, MN 55455, USA*

Received 17 July 2001; received in revised form 18 October 2001; accepted 19 October 2001

Abstract

Submicron magnetite crystals with mean sizes of 0.037, 0.10 and 0.22 μm undergo major changes in hysteresis properties and domain states in crossing the Verwey transition ($T_V \approx 120$ K). The 0.037 μm crystals are single-domain (SD) both in the cubic phase at room temperature T_0 and in the monoclinic phase below T_V. The 0.10 and 0.22 μm crystals have a mixture of SD and two-domain (2D) states at room temperature T_0, but mainly SD structures below T_V, in agreement with micromagnetic calculations. Coercive force H_c increases on cooling through T_V, by a factor 3–5 in the submicron magnetites and 40 in a 1.3 mm single crystal, because of the high crystalline anisotropy and magnetostriction of monoclinic magnetite. As a result, domain walls and SD moments are so effectively pinned below T_V that all remanence variations in warming or cooling are reversible. However, between ≈ 100 K and T_0, remanence behavior is variable. Saturation remanence (SIRM) produced in monoclinic magnetite at 5 K drops by 70–100% in warming across T_V, with minor recovery in cooling back through T_V (ultimate levels at 5 K of 23–37% for the submicron crystals and 3% for the 1.3 mm crystal). In contrast, SIRM produced in the cubic phase at 300 K decreases 5–35% (submicron) or $>95\%$ (1.3 mm) during cooling from 300 to 120 K due to continuous re-equilibration of domain walls, but there is little further change in cooling through T_V itself. However, the submicron magnetites lose a further 5–15% of their remanence when reheated through T_V. These irreversible changes in cycling across T_V, and the amounts of the changes, have potential value in determining submicron magnetite grain sizes. The irreversibility is mainly caused by 2D→SD transformations on cooling through T_V, which preserve or enhance remanence, while SD→2D transformations on warming through T_V cause remanence to demagnetize. © 2002 Elsevier Science B.V. All rights reserved.

Keywords: magnetite; hysteresis; magnetic domains; coercivity; remanent magnetization

1. Introduction

There has been much recent interest in the properties of magnetite at low temperatures, particularly in cycling through the Verwey transition ($T_V \approx 120$ K), where magnetite transforms from cubic to monoclinic structure [1–10]. Most published data (e.g. [2,4,11,12]) are for remanences produced in cubic magnetite at room temperature T_0, then cooled through T_V and warmed back to T_0. Only rarely (e.g. [13], Fig. 7; [14], Fig. 2; [8],

* Corresponding author. Tel.: +1-905-828-3829; Fax: +1-905-828-5425.
E-mail address: ozdemir@physics.utoronto.ca (O. Özdemir).

0012-821X/02/$ – see front matter © 2002 Elsevier Science B.V. All rights reserved.
PII: S0012-821X(01)00562-3

Fig. 5) have companion data been measured for remanences produced in the monoclinic phase below T_V, then warmed through T_V to T_0 and cooled back through T_V to the original temperature. Very few of these data are for submicron magnetites or large single crystals. One purpose of the present study was to produce high-quality hysteresis and remanence cycling data for these very small and very large magnetites.

Despite the wealth of published work, it is still unclear what controls the transformation of remanence across the cubic–monoclinic phase transition, or indeed what is the domain structure of monoclinic magnetite below T_V. Moloni et al. [3] were successful in imaging domains between 77 and 110 K on the {110} plane of discs cut from a large synthetic single crystal of magnetite, using a novel low-temperature magnetic force microscope. They found two types of domains, both typical of substances with strong uniaxial anisotropy. Lamellar domains without closure structures characterized parts of the crystal where the monoclinic *c*-axis (the easy axis of magnetization) lay in the plane of view, while intricate wavy patterns appeared in twinned regions where the *c*-axis intersected the viewing plane. Structures unfortunately faded from view around 110 K, but reappeared on cooling. Pinning of a wall by a topographic feature was observed in one case. No observations were possible of domains above T_V, nor of how structures transform or are renucleated between the cubic and monoclinic phases.

There are no domain observations at low temperatures for smaller magnetite crystals, but Muxworthy and Williams [15,16] have made micromagnetic calculations of the structures of model magnetite cubes ranging in size from 0.08 to 0.6 μm at temperatures down to 100 K. Modeling at lower temperatures was limited by fragmentary knowledge of the governing physical constants. One important prediction of their work is that the critical SD size increases from 0.07 μm in the cubic phase at T_0 to 0.14 μm in the monoclinic phase at 110 K, just below T_V. Thus we would expect to see a marked change in magnetic properties such as hysteresis parameters of magnetites in the 0.07–0.14 μm size range in crossing the Verwey transition. Testing this prediction is another purpose of our work.

2. Sample characterization

We studied three fine-grained magnetites with median particle sizes of 0.037, 0.10 and 0.22 μm. Their basic properties have been described by Dunlop [17,18]. The cube-shaped crystals were grown from aqueous solution and were initially surface oxidized. We therefore heated the magnetites in a mixture of 80% CO_2 and 20% CO for 120 h at 395°C to reduce the surface layer and then stored them in a desiccator until beginning experiments. Experimental samples were 2% by weight dispersions of magnetite in non-magnetic CaF_2.

Susceptibility curves measured with a Kappa bridge gave magnetite Curie temperatures of 575–580°C. X-ray unit cell edges determined using a Debye-Scherrer camera with Cu-Kα radiation were 8.393 ± 0.008, 8.399 ± 0.005 and 8.400 ± 0.005 Å for the 0.037, 0.10 and 0.22 μm samples, respectively. These values are characteristic of stoichiometric magnetite. Saturation magnetization M_s values of 85.8, 89.2 and 89.4 Am^2/kg (Table 1) also indicate nearly stoichiometric Fe_3O_4.

For comparison, we studied a 1.3 mm single

Table 1
Values of hysteresis parameters measured at room temperature and at low temperature

Grain size	Measurements at 295 K				Measurements at ≈15 K			
(μm)	M_s (Am^2/kg)	M_{rs}/M_s	H_c (mT)	H_{cr}/H_c	M_s (Am^2/kg)	M_{rs}/M_s	H_c (mT)	H_{cr}/H_c
0.037 ± 0.015	85.8	0.276	17.5	1.61	91.5	0.517	89.7	1.45
0.10 ± 0.03	89.2	0.219	13.3	1.64	95.4	0.406	50.2	1.28
0.22 ± 0.04	89.4	0.126	8.8	2.69	94.0	0.389	37.1	1.27
1300	90.7	0.003	0.13	45	–	0.013	1.1	–

crystal of magnetite from Richmond County, QC, Canada. The Curie temperature of 577°C, spinel unit cell edge $a = 8.397$ Å, and room temperature M_s of 90.7 Am^2/kg indicate stoichiometric magnetite with no major impurities.

3. Low-temperature hysteresis

Hysteresis loops were measured in a maximum field of 1.5 T at selected temperatures from ≈15 K to 295 K using a Princeton Measurements Corporation AGFM (MicroMag Model 2900) with a liquid He cryostat. Condensation and icing on the cryostat interfered with measurements below ≈15 K. Hysteresis measurements on the 1.3 mm crystal used a Quantum Design MPMS-2 SQUID magnetometer at Kyoto University, Japan.

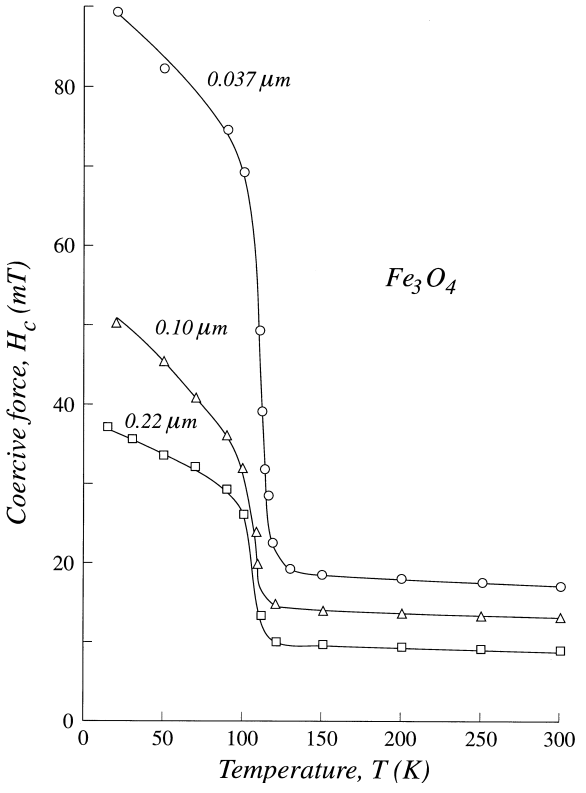

Fig. 1. Coercive force H_c measured in 1.5 T hysteresis loops at temperatures from ≈15 to 295 K. H_c is almost temperature independent above T_V, then increases sharply in crossing the Verwey transition for all submicron magnetites.

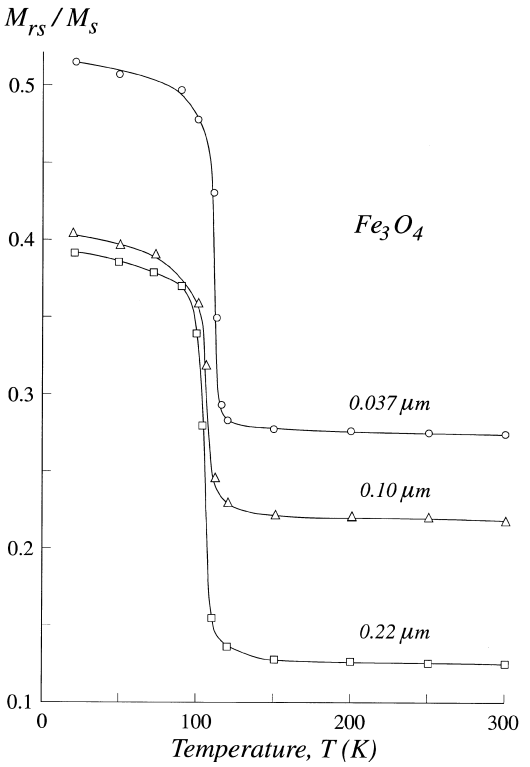

Fig. 2. Remanence ratios M_{rs}/M_s measured at low temperatures. Above T_V, M_{rs}/M_s is constant, indicating no change in domain state. Below T_V, all the submicron magnetites show sharp increases in M_{rs}/M_s, reaching SD-like values of 0.39–0.52 at ≈15 K.

Table 1 summarizes 295 K and ≈15 K values of the saturation magnetization M_s, saturation remanence to saturation magnetization ratio M_{rs}/M_s, coercive force H_c, and remanent to ordinary coercive force ratio H_{cr}/H_c. At ≈15 K, the three submicron samples have parameters approaching those of single-domain (SD) grains: $M_{rs}/M_s = 0.389$–0.517 and $H_{cr}/H_c = 1.27$–1.45. At 295 K, on the other hand, M_{rs}/M_s values are much below 0.5 and depend strongly on grain size, while H_{cr}/H_c increases to 1.6–2.7. H_c values are a factor 4–5 higher at ≈15 K than at room temperature.

Values of H_c for the submicron magnetites at intermediate temperatures are plotted in Fig. 1. Between room temperature and the onset of the

Verwey transition at $T_V \approx 120$ K, H_c is almost constant. Only for the 0.037 μm sample is there a slight increase, from 17.5 mT at 295 K to 19.0 mT at 130 K. This small gradual increase in H_c may reflect residual non-stoichiometry in the surface layers of these ultrafine magnetite crystals. The 0.037 μm sample had slightly lower M_s values than those of the other magnetites (Table 1), indicating some surface oxidation.

At the Verwey transition, all the submicron magnetites showed an increase in coercive force. The largest increase in H_c, from 20 mT at 125 K to 70 mT at 100 K, was for the 0.037 μm sample. Below 100 K, H_c continued to increase but more slowly, ultimately reaching 90 mT for the 0.037 μm sample at 20 K.

M_{rs}/M_s changes somewhat differently at low temperature (Fig. 2). As with H_c, M_{rs}/M_s values are almost temperature independent between 300 K and T_V. However, M_{rs}/M_s then increases very strongly and rapidly over the narrow temperature range 120–110 K, but unlike H_c, changes very little between 100 and 20 K for all the submicron samples. M_{rs}/M_s approximately doubled in cross-

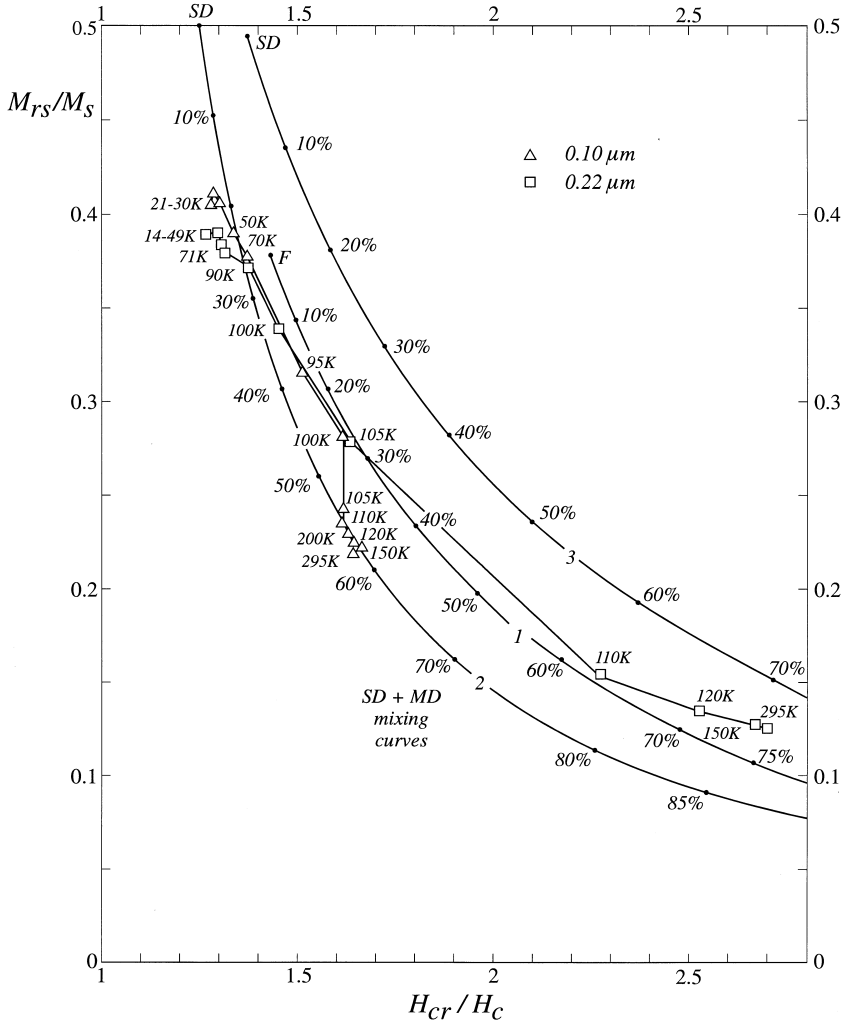

Fig. 3. Low-temperature hysteresis parameters of the 0.10 and 0.22 μm magnetites on a Day plot of M_{rs}/M_s vs. H_{cr}/H_c. The data follow PSD type curves [20] quite closely. Changes from more MD-like to SD-like parameters occur between 100 and 120 K (Verwey transition).

ing the Verwey transition for the 0.037 μm sample. The change in M_{rs}/M_s was largest of all for the 0.22 μm sample: from 0.136 at 120 K to 0.34 at 100 K.

The changing domain structure at low temperature is traced in Fig. 3 on a Day et al. [19] plot of M_{rs}/M_s vs. H_{cr}/H_c. The three type curves, calculated by mixing experimental data from SD (or fine-grained, F) and small multidomain (MD) end members, fit measured values for sized pseudo-single-domain (PSD) magnetites quite well [20]. The largest change in domain structure is for the 0.22 μm sample. At 150–295 K, $M_{rs}/M_s = 0.126$–0.128 and $H_{cr}/H_c = 2.66$–2.69, characteristic of moderately large PSD magnetites (70–75% MD mixtures), while at 14–71 K, $M_{rs}/M_s = 0.380$–0.389 and $H_{cr}/H_c = 1.27$–1.31, close to SD values. M_{rs}/M_s and H_{cr}/H_c hardly change on cooling through the isotropic temperature $T_i \approx 130$ K, where the first magnetocrystalline anisotropy constant K_1 changes sign and momentarily vanishes, in spite of the change at T_i from ⟨111⟩ to ⟨100⟩ easy axes which must cause some reorganization of the domains. M_{rs}/M_s and H_{cr}/H_c change mainly between 120 and 90 K, with ≈75% of this change (measured along the Day plot curves) occurring between 110 and 100 K. Changes in domain structure are therefore mainly a result of the decreasing lattice symmetry (cubic spinel → monoclinic) and accompanying large increase in crystalline anisotropy in crossing the Verwey transition. The changes in M_{rs}/M_s and H_{cr}/H_c are less dramatic for the 0.10 μm sample but again occur almost entirely at and below T_V, not around T_i.

The room temperature hysteresis curve of the 1.3 mm magnetite crystal is ramp-like and typical of large MD grains. Room- temperature hysteresis parameters are consistent with truly MD behavior: $M_s = 90.7$ Am^2/kg, $H_c = 0.13$ mT, $M_{rs}/M_s = 0.003$ and $H_{cr}/H_c = 45$. The temperature dependence of coercive force during cooling from 300 to 15 K is shown in Fig. 4. In contrast to the behavior of the submicron magnetites, H_c decreased on cooling, reaching a minimum at the isotropic temperature $T_i = 130$ K. In crossing the Verwey transition, H_c increased more than an order of magnitude, from 35 μT to 1.1 mT. The

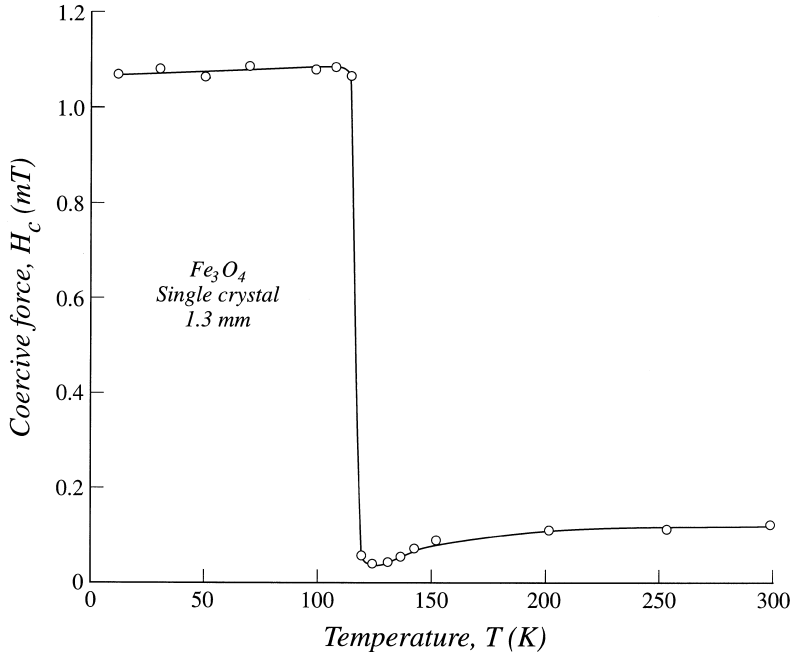

Fig. 4. Coercive force H_c measured in 0.4 T hysteresis loops for the 1.3 mm crystal of magnetite at temperatures from 10 to 300 K.

change was much sharper than for the submicron magnetites, occurring mainly in a <10 K interval below 120 K. In cooling from 110 to 15 K, H_c remained essentially constant, again in contrast to the submicron magnetites.

4. Isothermal remanence cooling (300→5 K) and warming (5→300 K) curves

We measured temperature dependence of remanence with an MPMS-2 SQUID magnetometer at the Institute for Rock Magnetism, University of Minnesota, Minneapolis, MN, USA. Samples were given a saturation isothermal remanent magnetization (SIRM) in a field of 2.5 T at room temperature, then cooled in zero field to 5 K and back to 300 K. The SIRM cooling and warming curves for the submicron magnetites are shown in Fig. 5. The SIRM cooling curve for the 0.037 μm sample is almost flat between 300 and 150 K. In further cooling across the Verwey transition, the remanence dropped to 95% of the original SIRM, but this was not a permanent demagnetization. SIRM cooling and warming curves were reversible for the monoclinic phase in the range 5–90 K, with all but 2% of the initial SIRM intensity being recovered at 5 K. Warming through the Verwey transition resulted in a permanent remanence loss, however, with $\approx 85\%$ of the original SIRM remaining at 300 K.

In cooling from 300 K to T_V, the remanence of the 0.10 μm magnetite decreased in much the same way as that of the 0.037 μm magnetite. At T_V, 10% of initial SIRM had apparently been demagnetized but all but 2% of this remanence was recovered in cooling to 5 K. The remanence retraced the cooling curve in warming from 5 to 100 K, then decreased sharply at the monoclinic→cubic phase transition. The memory at room temperature was about 80% of the initial SIRM.

The zero field cooling and warming curves of SIRM for the 0.22 μm sample had many of the same features as those of 0.037 and 0.10 μm magnetites but the decrease in remanence with cooling to T_V was larger. At the phase transition, the remanence was only 63% of the initial SIRM

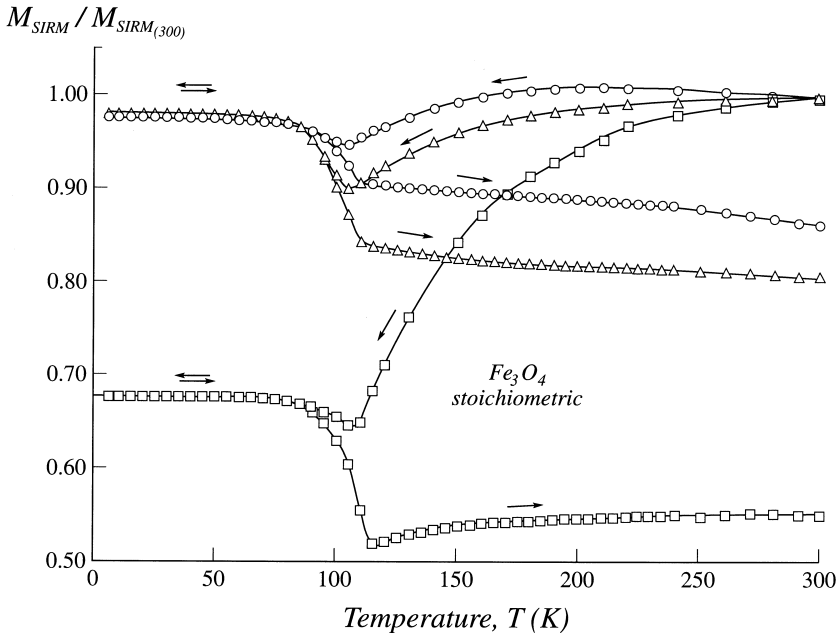

Fig. 5. Normalized temperature variation of saturation isothermal remanence (SIRM) of submicron magnetites during zero field cooling from 300 to 5 K and zero field warming back to 300 K. SIRM was produced in a field of 2.5 T at 300 K. Open circles, triangles and squares represent the 0.037, 0.10 and 0.22 μm magnetites, respectively.

and there was little recovery in cooling to 5 K. The cooling and warming curves below T_V resemble those of the 0.037 and 0.10 μm samples. In warming from 90 to 120 K, the remanence decreased a further ≈15%, then increased slightly with further warming. At 300 K, the surviving remanence was 55% of the original SIRM.

For all submicron magnetites, SIRM cooling and warming curves are irreversible for the high-temperature cubic phase but completely reversible at all temperatures below 90 K for the low-temperature monoclinic phase. The remanence decrease across the Verwey transition during the warming half cycle becomes more marked with increasing grain size. The permanent remanence loss at 300 K after a complete cycle also increases with increasing grain size.

SIRM cooling and warming curves for the 1.3 mm magnetite crystal appear in Fig. 6. The remanence decreased steadily with cooling to the Verwey transition, as for the 0.22 μm magnetite, but the changes were much larger. By 120 K, only 3% of the original SIRM remained. The remanence then increased sharply in cooling across T_V, followed by a smaller more gradual decrease between 110 and 100 K. In warming from 10 K to T_V, the behavior was completely reversible, but above T_V, the remanence did not retrace the cooling curve but increased slightly until 150 K and then became almost temperature independent. The SIRM memory at room temperature was ≈10%.

5. Isothermal remanence warming (5→300 K) and cooling (300→5 K) curves

The submicron magnetites were cooled to 5 K in zero field, where they were given a 2.5 T SIRM, and then warmed to 300 K in zero field. The shapes of the remanence curves between 5 and 90 K and also across the Verwey transition were basically the same for all samples, but the amount of remanence lost at T_V increased with increasing grain size (Fig. 7). In warming from 5 K, there was a slight drop in remanence extending up to 35 K for all the submicron magnetites. Similar behavior has been observed for a large natural single crystal of magnetite by Özdemir et al. [1], ruling out remanence unblocking in ultrafine par-

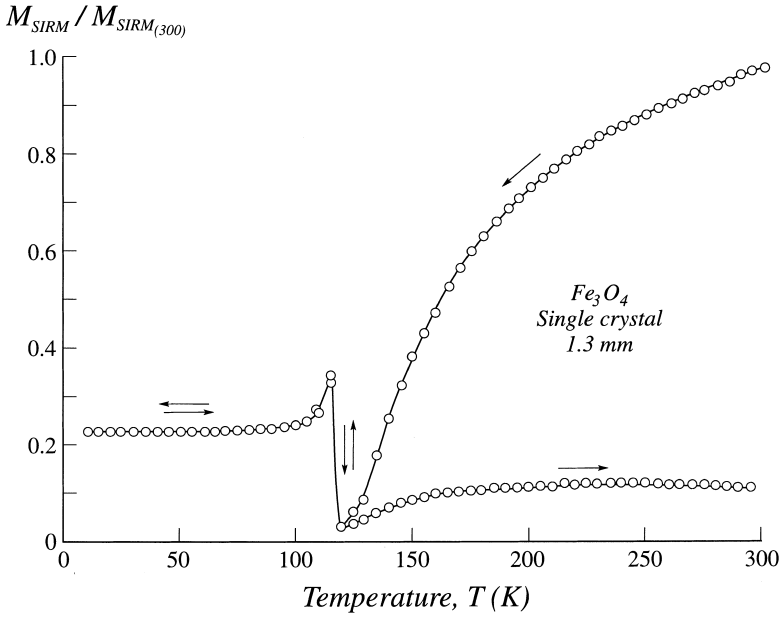

Fig. 6. Normalized zero field cooling (300→5 K) and warming (5→300 K) curves for SIRM produced at 300 K in the 1.3 mm crystal of magnetite.

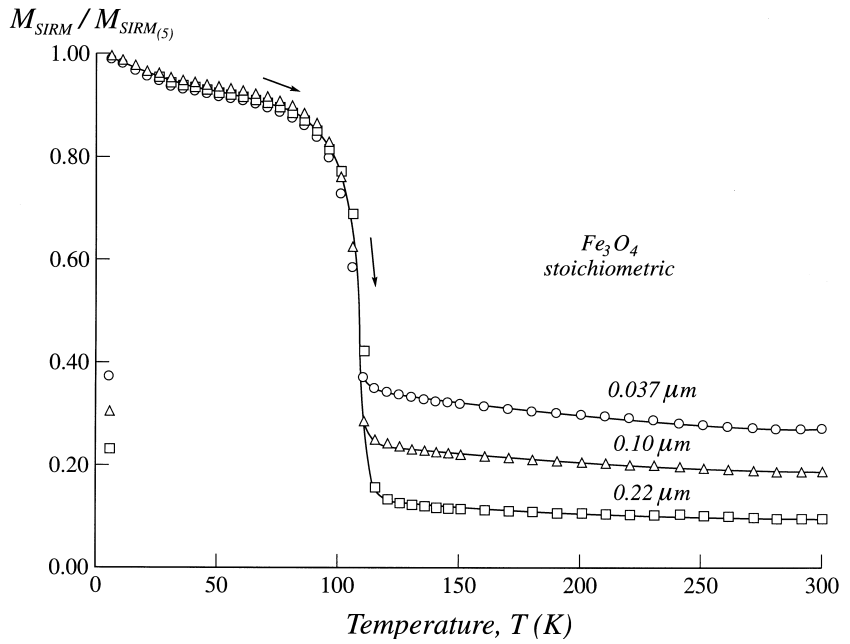

Fig. 7. Normalized zero field SIRM warming curves from 5 to 300 K for submicron magnetites. SIRM was produced in monoclinic magnetite in a field of 2.5 mT at 5 K. The open circle, triangle and square at 5 K are SIRM memories after a complete warming–cooling cycle.

ticles as a cause. The remanence drop may be related to a 30–35 K transition, marked by a sharp peak in the quadrature susceptibility k'' at this temperature [21,22]. Following major drops at the Verwey transition, the remanence remained constant or decreased slightly in warming above T_V. In recooling across the Verwey transition, there was little recovery of low-temperature remanence. The SIRM memories for the 0.037, 0.10 and 0.22 μm samples at 5 K were 37, 31 and 23% of the original monoclinic SIRM, respectively.

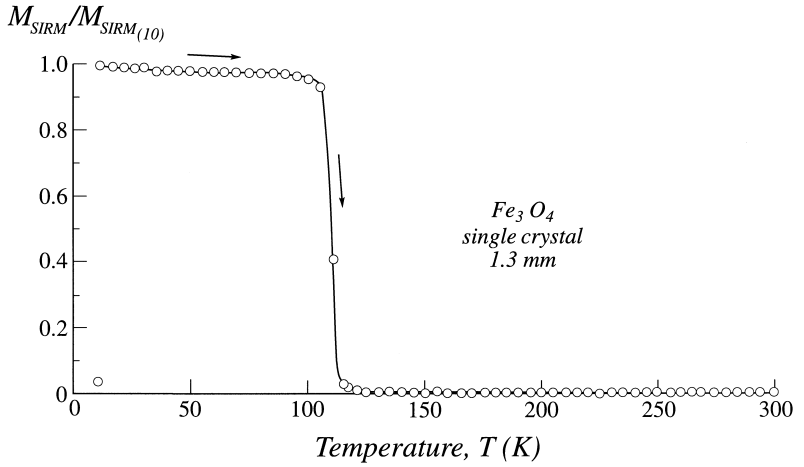

Fig. 8. Normalized zero field SIRM warming curve from 10 to 300 K for the 1.3 mm crystal of magnetite. The single point at 10 K is the SIRM memory of monoclinic magnetite after cooling from 300 to 10 K.

The SIRM warming curve for the 1.3 mm magnetite crystal (Fig. 8) differs in several ways from the submicron magnetite curves. The remanence was almost temperature independent between 10 and 100 K. At the crystallographic phase transition, the remanence decreased abruptly over only two temperature steps to practically zero, where it remained from T_V to 300 K. Thus SIRM produced in monoclinic magnetite of this size is completely demagnetized in the transition to the cubic phase. Almost no memory of the initial SIRM was recovered in recooling through the Verwey transition.

6. Discussion

6.1. Domain states at room temperature and low temperature

Magnetite in 0.037 μm cubes should have SD structure both above and below T_V. We measured $M_{rs}/M_s = 0.517$ at ≈ 15 K, but at 295 K, M_{rs}/M_s was only 0.276 (Table 1). A major factor in this difference is superparamagnetism. Particles have a distribution of sizes about the mean and the smaller particles are thermally unstable or superparamagnetic (SP) at 295 K [17]. They contribute to M_s but not to M_{rs}, thereby lowering the M_{rs}/M_s ratio. At 15 K, most of these particles are stable SD because thermal energy kT is 20 times smaller. M_{rs}/M_s thus increases to more SD-like values. SP behavior at room temperature is probably responsible also for the rather high H_{cr}/H_c value of 1.61 [20].

Two factors influence the SD value of M_{rs}/M_s: 'flowering' of the spins at the corners of SD grains [23,24] and the number of easy axes of anisotropy. The flowering factor is 0.92 for 0.1 μm magnetite cubes [15] and increases with decreasing size [23]. More significant is the difference between uniaxial and multiaxial anisotropy. Perfect cubes at 295 K would have purely magnetocrystalline anisotropy with four equivalent ⟨111⟩ easy axes, leading to an expected M_{rs}/M_s of 0.866 ([25], Ch. 11). However, high-temperature hysteresis [26] suggests that there is sufficient elongation of our submicron cubes to make uniaxial shape anisotropy important; $M_{rs}/M_s = 0.5$ is expected for uniaxial anisotropy. Experimentally (Fig. 2) there is no obvious change in M_{rs}/M_s for any of the submicron magnetites in passing the isotropic temperature $T_i = 130$ K, where K_1 momentarily vanishes and the spins in perfect SD cubes would rotate to ⟨100⟩ easy axes, with $M_{rs}/M_s = 0.832$. Shape anisotropy is probably responsible.

The evolving domain structures of the 0.1 and 0.22 μm magnetites are well displayed in Fig. 3. At room temperature, both have PSD values of M_{rs}/M_s and H_{cr}/H_c which change to almost SD values at 15–50 K. Because 0.1 μm is above the critical SD size d_0 for cubic magnetite but below d_0 for monoclinic magnetite [15], this is the expected trend for our 0.1 μm magnetite. The trend for our 0.22 μm magnetites is not as expected, however. Such grains are well above the predicted d_0 of 0.14 μm at 110 K and should not have M_{rs}/M_s and H_{cr}/H_c values almost identical to those of the 0.1 μm magnetites at 15–50 K. Perhaps, as the H_c values in Fig. 1 suggest, the anisotropy of monoclinic magnetite increases enough with cooling from T_V to 50 K to push d_0 above 0.22 μm. Of course, the M_{rs}/M_s values of 0.406 and 0.389 at 15 K are distinctly lower than $M_{rs}/M_s = 0.517$ of the 0.037 μm sample, so there must be some compromise with SD structure in the larger grains, likely an admixture of two-domain (2D) states.

Values of M_{rs}/M_s and H_{cr}/H_c at room temperature and down to 150 K indicate quite different structures for 0.1 μm compared to 0.22 μm magnetites, but not as different as recent micromagnetic theories predict. In early modeling, Dunlop [17,27,28] proposed from several independent lines of evidence that 0.1 μm magnetites have essentially SD structure, whereas 0.22 μm magnetites have 2D structure with a broad domain wall that fills a substantial fraction of the grain. Recent micromagnetic models come to similar conclusions. The SIRM state predicted for 0.1 μm cubes is essentially SD both above and below T_V, with only a slight difference in the degree of flowering, while 0.3 μm cubes have room temperature SIRM of $0.09–0.17 \times (M_{rs})_{SD}$ [15]. The observed 150–295 K values of M_{rs}/M_s are 0.219–0.223 for the 0.1 μm sample, lower than predicted,

and 0.126–0.128 for the 0.22 μm sample, higher than predicted. Both samples have wide size distributions. Probably the smaller grains in each sample are SD and the larger ones are in 2D/vortex states. The fraction of SD grains will be much greater in the 0.1 μm sample; hence its higher M_{rs}/M_s.

In all three submicron magnetites, most of the change in domain structure is accomplished over a very narrow temperature range and is clearly associated with the cubic→monoclinic phase change at the Verwey transition, not with the change of easy axes in the cubic phase at T_i. This is also the case for the 1.3 mm crystal, although there are smaller-scale minima in H_c and M_{rs}/M_s at T_i associated with the minimum in crystalline anisotropy at the isotropic point (Fig. 4).

Because of self-demagnetization, any change in H_c in an MD ferromagnet is expected to produce a proportional change in M_{rs} through adjustment of domain wall positions: $M_{rs} = H_c/N$, where N is demagnetizing factor ([25], Ch. 5). This is approximately true even for the profound changes in magnetic properties and domain structure that occur in crossing the Verwey transition [3,29]. From Table 1, H_c for our 1.3 mm crystal increases from 0.13 to 1.1 mT between 295 and ≈15 K, while M_{rs}/M_s increases by a similar factor, from 0.003 to 0.013. The ratio between H_c and M_{rs} (both expressed in A/m, 15 K data) is 0.18, which is comparable to $N = 0.33$ for an equidimensional crystal.

6.2. Low-temperature coercive force

From the temperature dependence of coercive force H_c, one can deduce the relative contributions of magnetocrystalline, magnetoelastic and shape anisotropies and hence what factor or factors control the stability of low-temperature remanence and room temperature memory. Shape anisotropy is indicated by $H_c(T) \propto M_s(T)$. For magnetocrystalline and magnetoelastic anisotropies the coercivity has a K_1/M_s or λ_s/M_s temperature dependence (λ_s is the isotropic magnetostriction), leading to a variation $H_c(T) \propto M_s^n(T)$ with $n > 1$.

Bilogarithmic plots of H_c vs. M_s for our submicron samples in the range 120–300 K were straight lines with slopes $n = 1.71$, 1.45 and 1.74 for the 0.037, 0.10 and 0.22 μm magnetites, respectively. The value of $n = 1.71$ for the 0.037 μm magnetite is not a reliable indicator of anisotropy because H_c is greatly affected by the reversed moment of the SP fraction. For the 0.10 and 0.22 μm magnetites, the variations $H_c(T) \propto M_s^{1.45}(T)$ and $M_s^{1.74}(T)$ reflect some combination of shape, magnetocrystalline and magnetoelastic anisotropies. At the isotropic point $T_i = 130$ K, H_c values for the three samples were 19.6, 14.5 and 9.8 mT, respectively, indicating a large contribution from shape and magnetoelastic anisotropies. If magnetocrystalline anisotropy were the main source of coercivity, H_c would have very small values at T_i, where K_1 becomes zero, as was the case for the 1.3 mm crystal (Fig. 4).

Cooling the submicron samples through the Verwey transition resulted in large increases in H_c, as much as a factor 3 for the 0.037 μm magnetite (Fig. 1). Increases in H_c in the vicinity of T_V have been observed previously [6,9,30–32], although the changes were only sharp for grain sizes ≥0.25 μm. H_c increases because of the large changes in magnetocrystalline and magnetoelastic anisotropies when magnetite deforms to monoclinic structure at T_V. Magnetocrystalline anisotropy constants, K_a, K_b, K_u, K_{aa}, K_{bb} and K_{ab} of monoclinic magnetite below T_V are much larger than K_1 of cubic magnetite [33]. Magnetostriction and magnetoelastic constants also increase discontinuously in the vicinity of T_V [34].

Muxworthy and Williams [16] used three-dimensional micromagnetic simulations to predict H_c values for 0.08–0.3 μm magnetites between 100 and 300 K. Below T_V, for all grain sizes magnetization reversals were by coherent rotation in the monoclinic easy plane. Very large H_c values were predicted for monoclinic magnetite. For 0.1 μm grains at 100 K, the model gave $H_c \approx 200$ mT. This theoretical value is 10 times larger than our experimental value of 20.8 mT at 100 K for the same grain size (Fig. 1). The disagreement between the experimental and theoretical values might be due to simplifications in the theoretical

model, for example, neglecting magnetostrictive and magnetoelastic anisotropies.

The temperature dependence of H_c for the 1.3 mm crystal is quite different from that of the submicron magnetites (Fig. 4). H_c decreases with cooling from 300 K to a minimum of 0.035 mT around $T_i = 130$ K. Recent work on natural single crystals of magnetite has shown that H_c varies with temperature as λ_s/M_s between 300 and 170 K, indicating the importance of magnetoelastic anisotropy over this temperature range [7]. Coarse-grained magnetites behave similarly [35]. Below 170 K, the coercivity is controlled by magnetocrystalline anisotropy as well [7], and this accounts for the marked minimum at 130 K. In crossing the Verwey transition, H_c increases very sharply by almost a factor 40.

6.3. Low-temperature cycling of SIRM

The variation of remanence during a low-temperature cycle depends strongly on the temperature at which the remanence was produced and the consequent direction of approach to T_V. In both our submicron and mm size crystals of magnetite, if SIRM is given to the monoclinic phase at low temperature and T_V is approached from below, a major part of the remanence is lost at the phase transition (Figs. 7, 8). Most of the decrease at T_V is permanent, with almost no recovery in the second crossing of the Verwey transition in the cooling half of the cycle for the 1.3 mm crystal and 23–37% recovery for the submicron magnetites. The shape of the curves is almost independent of grain size, except for the memories. On the other hand, if SIRM is imparted to the cubic phase at room temperature T_0 and T_V is approached from above, the memories and the shapes of the demagnetization curves are strongly dependent on the domain state and grain size (Figs. 5, 6).

The temperatures at which demagnetization occurs are also strongly controlled by the type of low-temperature cycling. For example, if the SIRM is induced at low temperatures and T_V is approached from below, almost total demagnetization occurs at T_V. In this case, the isotropic point T_i is unimportant (Figs. 7, 8). If SIRM is induced at T_0 and T_V is approached from above, T_i and T_V both play an important role in the demagnetization mechanism [2,5]. The first demagnetization occurs at T_i because the isotropic point must be passed on the way to T_V. This is particularly important for remanences carried by PSD and MD magnetites, in which magnetocrystalline anisotropy controls a major part of the remanence.

There are two reasons to expect differences between the results of cooling–warming and warming–cooling cycles. First, the domain structure of monoclinic magnetite below T_V is different from that of cubic magnetite above T_V [3,29]. Below T_V, spins lie along the [001] *c*-axis, domains are lamellar without closure structures, and walls are strongly pinned by crystal defects because of the high magnetostriction and crystalline anisotropy. Many submicron grains lack domain walls entirely, as Table 1 and Fig. 3 attest. Above T_V, spins have a choice of six or eight easy directions evenly distributed in space, promoting sets of domains with different orientations linked by closure structures, and walls are less strongly pinned, particularly near T_i. Thus the starting remanence has very different properties. Second, as mentioned above, in cooling–warming cycles domains must pass T_i before reaching T_V, whereas in warming–cooling cycles, profound changes have already occurred at T_V before T_i is reached.

We will discuss first the results of our cooling–warming cycles of SIRM. This process is often referred to as low-temperature demagnetization (LTD), although it has seldom been used as a routine paleomagnetic cleaning technique [36–39]. There is some ambiguity in what is meant by magnetic memory in low-temperature cycling. In the first passage of the Verwey transition, a certain fraction of the initial remanence survives (or is recovered after a dip at T_V itself): this is the 'first memory'. The fraction of the initial remanence remaining after the second passage of T_V is the 'second memory'. When LTD is done for paleomagnetic purposes, usually only the second memory is measured. King and Williams [9] argue that a more logical definition of memory is the fraction of room-temperature remanence recovered after a complete cycle, i.e. second memory−

first memory (their Fig. 10). For our results (Figs. 5 and 6), this quantity is negative: on second passage of T_V, there is a further loss of remanence, not a recovery, and the second memory cannot be taken as a baseline remanence that is unaffected by passage through T_V. Yet there is remanence recovery, as shown by dips and recoveries at T_V in one or both passages (Figs. 5, 6).

6.4. Cooling+warming cycles of SIRM

Cooling through the Verwey transition has little effect on room-temperature SIRM for the 0.037 μm magnetite sample, apart from a minor dip and recovery at T_V itself (Fig. 5), probably because the SD remanence in this sample is controlled mainly by shape anisotropy. For the 0.10 and 0.22 μm magnetites, at least some of which contain walls or wall-like vortex structures above T_V, there are increasing remanence losses in cooling from T_0 to T_V but these are not localized near T_i. Wall unpinning is likely responsible because the demagnetization is much less in the 0.10 μm grains than in the 0.22 μm grains where 2D structures are more prevalent. However, there is no important change in remanence in the first crossing of the Verwey transition apart from a mild recovery which is most marked for the 0.10 μm grains. In cooling and rewarming below T_V, the remanence is constant until around 90 K, when a substantial further demagnetization occurs in the second passage of T_V.

The behavior of the 1.3 mm crystal is different in several respects (Fig. 6). The amount of demagnetization in cooling from T_0 to T_V is much greater ($>90\%$) and there is an inflection around 130 K matching the minimum in H_c at the same temperature (Fig. 4). These differences are a natural consequence of progressive wall unpinning. The numerous domain walls in this large crystal have much more freedom of movement than the single walls in submicron grains. Another difference is the large and sudden increase in remanence on cooling through T_V, which is matched by an equal decrease in rewarming through the transition. In the submicron magnetites, reversible changes were confined to temperatures below 90 K and behavior across T_V was highly irreversible.

The contrasting responses of large and small magnetites in crossing the Verwey transition may be related to monoclinic twinning. As a magnetite crystal cools through T_V, the unit cell distorts from cubic to monoclinic. If all parts of the crystal have the same monoclinic *c*-axis, the entire crystal must distort. To reduce such megascopic strain, different parts of the crystal tend to form twins with different *c*-axes [40,41] and contrasting domain patterns [3]. Strain is accommodated at the boundaries between twinned regions, which are consequently under stress [42]. The spacing between twin boundaries, dictated by the requirement that overall crystal strain be minimized, is between 0.3 and 2 μm. Thus below T_V, our 1.3 mm crystal contains numerous monoclinic twins whereas the submicron magnetite crystals are probably untwinned.

The stressed twin boundaries and twin junctions (where twins oriented at right angles meet) act as strong pinning sites for magnetic domain walls. In crossing the Verwey transition, domain wall thickness decreases sharply because of the abrupt increases in magnetocrystalline and magnetostriction constants [5] and this increases the efficiency with which the walls are pinned [43,44]. In recrossing the Verwey transition, the crystal reverts to cubic structure, the twin boundaries disappear and the remanence decreases reversibly to its original level in the 1.3 mm crystal (Fig. 6). Submicron magnetites are untwinned and lack this lock-in mechanism ensuring reversible behavior in cycling across the transition.

Why do the submicron magnetites scarcely change their remanence intensity in cooling through T_V but lose substantial remanence on rewarming through T_V? First, pinning of walls to crystal defects such as dislocations which exist both above and below T_V increases on cooling through the transition but decreases on warming. Demagnetization associated with wall unpinning will occur on warming, not cooling. Second, SD structures predominate in all submicron samples in the monoclinic phase. In the 0.037 μm grains, both cubic and monoclinic phases are SD, and shape anisotropy evidently bridges the transition (Fig. 5). In the 0.10 and 0.22 μm grains, judging by their higher *n* values, shape anisotropy is less

influential. In cooling, the easy axis above T_V, which lies within a cone around the SIRM direction, becomes the SD *c*-axis below T_V and remanence is preserved (or could even increase if 2D→SD, accounting for the dip and recovery phenomenon). On rewarming through T_V in zero field, the choice of multiple easy axes disperses the remanence of grains that remain SD, while those grains that nucleate a wall demagnetize. With increasing grain size, the role of multiaxial anisotropy grows and the proportion of 2D grains increases, with the result that remanence loss across the transition increases (Fig. 5).

Micromagnetic simulations of SIRM cooling–warming curves for model 0.3 μm magnetite cubes by Muxworthy and Williams ([15], Fig. 14) reproduce many of the features of our 0.22 μm results. The progressive demagnetization in cooling from T_0 to T_V is predicted to be ≈60%, whereas we observe ≈35% loss for our somewhat smaller grains. There is a small dip and recovery of remanence in crossing the transition, and constant reversible behavior in cooling and rewarming below ≈100 K, both as observed. The warming curve across the transition has a further irreversible loss of remanence, but the magnitude is only one half of the 15% we observe. Finally there is only minor recovery above T_V: both their theoretical and our experimental remanence curves are almost flat from 120 K to T_0. This good agreement between theory and observations is most encouraging.

6.5. Warming+cooling cycles of SIRM

The behavior of SIRM of monoclinic magnetite in warming–cooling cycles across T_V is quite unlike that of SIRM of cubic magnetite in cooling–warming cycles. Room temperature SIRM demagnetizes in cooling to T_V, by amounts that increase with increasing grain size (Figs. 5, 6) but SIRM imparted at 5 K scarcely changes with heating until T_V is reached, and the curves are grain size independent (Figs. 7, 8). The strong uniaxial anisotropy of monoclinic magnetite must be responsible for pinning domain walls in the larger grains and SD moments in small grains. The 2.5 T field applied at 5 K aligns spins along the monoclinic *c*-axis in each submicron crystal and the spins are locked in along [001] when the field turned off.

In crossing the phase transition, permanent demagnetization of all the magnetites occurs at T_V when the crystal structure changes from monoclinic to cubic. The amount of demagnetization for the submicron magnetites is much greater than the corresponding demagnetization of room temperature SIRM memory when it was warmed across T_V (Figs. 5, 7). In warming through and above T_V, there is no dip and recovery of remanence like that seen in cooling the room temperature SIRM through T_V. The Verwey transition is all important in warming monoclinic SIRM; there is no expression of T_i in the remanence variation. Furthermore, the large amounts of demagnetization that occurred in cooling the room temperature SIRM of the submicron magnetites from T_0 to T_V are completely lacking in the monoclinic SIRM memory over the same range.

All these observations force us to the conclusion that the memory of cubic phase SIRM below the Verwey transition has a domain state entirely different from that of SIRM produced directly in the monoclinic phase at low temperature. The converse is equally true: memory of monoclinic SIRM transformed to the cubic phase is not at all equivalent in its properties to SIRM imparted to the cubic phase above T_V.

Although we do not yet understand the domain structure of monoclinic magnetite well enough to interpret these differences in detail, the contrasting magnetic properties of SIRM warming–cooling cycles and cooling–warming cycles could be useful in diagnosing the presence and grain size of magnetite in natural materials such as sediments and soils. Warming curves of low-temperature monoclinic phase SIRM are routinely used to detect magnetite in environmental studies, and they clearly provide a very sharp indication of the Verwey transition (Figs. 7, 8). On the other hand, cooling–warming curves of room-temperature cubic phase SIRM provide a wealth of details not present in the monoclinic warming curves (Fig. 5, 6), including several key indicators of grain size and domain structure.

The first size indicator is the second memory,

which ranges from 86% for 0.037 μm grains to 80% for 0.10 μm and 55% for 0.22 μm grains. The second indicator is the loss of remanence in cooling from T_0 to T_V, which is 5% for 0.037 μm, 10% for 0.10 μm and 35% for 0.22 μm grains. Finally, the change in remanence in warming across T_V (approximately equal to first memory−second memory) is $\approx$5% for 0.037 μm, $\approx$12% for 0.10 μm, and $\approx$15% for 0.22 μm grains. The corresponding range of memories for monoclinic SIRM is 23–37% (Fig. 7), offering less potential size resolution.

7. Conclusions

Submicron magnetites undergo important changes in their hysteresis properties and domain states in crossing the Verwey transition. Our smallest crystals (0.037 μm) are SD/SP at room temperature T_0 ($M_{rs}/M_s = 0.276$, $H_c = 17.5$ mT) but thermally stable SD at 15 K ($M_{rs}/M_s = 0.517$, $H_c = 90$ mT) (Table 1, Figs. 1, 2). Larger crystals have PSD parameters at T_0 ($M_{rs}/M_s = 0.219$, 0.10 μm; $M_{rs}/M_s = 0.126$, 0.22 μm) but almost SD properties at 15 K ($M_{rs}/M_s = 0.406$, 0.10 μm; $M_{rs}/M_s = 0.389$, 0.22 μm) (Fig. 3), and probably contain a mixture of SD and 2D/vortex states. These observations are in approximate agreement with micromagnetic predictions [15,16].

Coercive force H_c increases by factors of 3–40 between 120 and 100 K, and continues to increase with further cooling in the submicron magnetites (Table 1, Figs. 1, 4). The increases reflect the large increases in magnetocrystalline anisotropy and magnetostriction in the cubic→monoclinic phase transition. Although the increases are large, for the submicron magnetites they are only $\approx$10% of the increase in H_c predicted by micromagnetic modeling [16].

Low-temperature cycling results are very different depending on whether SIRM is produced in the monoclinic phase and heated through T_V or produced in the cubic phase and cooled through T_V. One reason is the different domain structures of monoclinic and cubic magnetites, and transformations between the structures across T_V (e.g. SD→2D in warming, 2D→SD in cooling). Another reason is the very high anisotropy and coercivity below T_V, which pins both domain walls and SD moments tightly, compared to the weaker anisotropy above T_V, which permits continuous re-equilibration of domain walls during cooling from T_0.

There are some novel features in cooling–warming cycles of cubic phase SIRM which have not been previously reported. There is only a slight dip and recovery of remanence between 120 and 100 K in cooling, but a major permanent loss of remanence in rewarming from 100 to 120 K, which increases with increasing grain size. One cause is the change of crystalline anisotropy from uniaxial to multiaxial in the monoclinic→cubic transformation, which disperses the remanence. Even more important is the SD→2D/vortex transformation across the transition. In our 1.3 mm crystal, there are large remanence changes across the transition but these are perfectly reversible because domain walls are firmly locked in place by *c*-axis twin boundaries in the monoclinic phase.

Warming–cooling cycles of monoclinic phase SIRM are simpler, with $>$50% loss of remanence in the first crossing of the Verwey transition, almost constant remanence above T_V, and only minor recovery in the second crossing. The very large permanent remanence losses in submicron grains are not easy to explain in view of the much smaller and very size-dependent losses seen in the cooling half cycle of the cubic phase SIRM. The monoclinic and cubic SIRMs must involve entirely different domain structures, even after transformation across T_V.

Although warming curves of monoclinic SIRM are conventionally used to identify magnetite in rocks, sediments and soils, cooling–warming cycles of cubic phase SIRM offer three grain size diagnostic indicators for submicron magnetites. These are remanence loss in cooling from 300 to 120 K, further remanence loss in warming from 100 to 120 K (second crossing of T_V), and ultimate remanence level or memory after a complete 300→10→300 K cycle. Monoclinic SIRM memory is a less sensitive indicator of submicron grain sizes.

Acknowledgements

We are grateful to Prof. M. Torii for help with the measurements at Kyoto University. The Institute for Rock Magnetism, University of Minnesota, Minneapolis, MN, USA is operated with support from NSF and the Keck Foundation. The 1.3 mm magnetite crystal was kindly donated by M. Back of the Royal Ontario Museum, Toronto, ON, Canada. We thank Subir Banerjee, Gunther Kletetschka and Valera Shcherbakov for helpful reviews. This research was supported by NSERC Canada through grant A7709 to D.J.D.*[RV]*

References

[1] Ö. Özdemir, D.J. Dunlop, B.M. Moskowitz, The effect of oxidation on the Verwey transition in magnetite, Geophys. Res. Lett. 20 (1993) 1671–1674.
[2] S.L. Halgedahl, R.D. Jarrard, Low-temperature behavior of single-domain through multidomain magnetite, Earth Planet. Sci. Lett. 130 (1995) 127–139.
[3] K. Moloni, B.M. Moskowitz, E.D. Dahlberg, Domain structures in single crystal magnetite below the Verwey transition as observed with a low-temperature magnetic force microscope, Geophys. Res. Lett. 23 (1996) 2851–2854.
[4] J.P. Hodych, R.I. Mackay, G.M. English, Low-temperature demagnetization of saturation remanence in magnetite-bearing dolerites of high coercivity, Geophys. J. Int. 132 (1998) 401–411.
[5] Ö. Özdemir, D.J. Dunlop, Low-temperature properties of a single crystal of magnetite oriented along principal magnetic axes, Earth Planet. Sci. Lett. 165 (1999) 229–239.
[6] A. Muxworthy, Low-temperature susceptibility and hysteresis of magnetite, Earth Planet. Sci. Lett. 169 (1999) 51–58.
[7] Ö. Özdemir, Coercive force of single crystals of magnetite at low temperatures, Geophys. J. Int. 141 (2000) 351–356.
[8] A. Muxworthy, E. McClelland, The causes of low-temperature demagnetization of remanence in multidomain magnetite, Geophys. J. Int. 140 (2000) 115–131.
[9] J.G. King, W. Williams, Low-temperature magnetic properties of magnetite, J. Geophys. Res. 105 (2000) 16427–16436.
[10] A. Kosterov, Magnetic hysteresis of pseudo-single-domain and multidomain magnetite below the Verwey transition, Earth Planet. Sci. Lett. 186 (2001) 245–254.
[11] R.L. Hartstra, A comparative study of the ARM and I_{SR} of some natural magnetites of MD and PSD grain size, Geophys. J. R. Astron. Soc. 71 (1982) 497–518.
[12] J.P. Hodych, Low-temperature demagnetization of saturation remanence in rocks bearing multidomain magnetite, Phys. Earth Planet. Inter. 66 (1991) 144–152.
[13] M. Ozima, M. Ozima, S. Akimoto, Low temperature characteristics of remanent magnetization of magnetite: Self-reversal and recovery phenomena of remanent magnetization, J. Geomagn. Geoelectr. 16 (1964) 165–177.
[14] K. Kobayashi, M. Fuller, Stable remanence and memory of multi-domain materials with special reference to magnetite, Philos. Magn. 18 (1968) 601–624.
[15] A.R. Muxworthy, W. Williams, Micromagnetic models of pseudo-single-domain grains of magnetite near the Verwey transition, J. Geophys. Res. 104 (1999) 29203–29217.
[16] A.R. Muxworthy, W. Williams, Micromagnetic calculation of hysteresis as a function of temperature in pseudo-single-domain magnetite, Geophys. Res. Lett. 26 (1999) 1065–1068.
[17] D.J. Dunlop, Superparamagnetic and single-domain threshold sizes in magnetite, J. Geophys. Res. 78 (1973) 1780–1793.
[18] D.J. Dunlop, Hysteresis properties of magnetite and their dependence on particle size: A test of pseudo-single-domain remanence models, J. Geophys. Res. 91 (1986) 9569–9584.
[19] R. Day, M. Fuller, V.A. Schmidt, Hysteresis properties of titanomagnetites: Grain size and composition dependence, Phys. Earth Planet. Inter. 13 (1977) 260–267.
[20] D.J. Dunlop, Theory and application of the Day plot (M_{rs}/M_s vs. H_{cr}/H_c) 1. Theoretical curves and tests using titanomagnetite data, J. Geophys. Res. 106 (2001) in press.
[21] B.M. Moskowitz, M. Jackson, C. Kissel, Low-temperature magnetic behaviour of titanomagnetites, Earth Planet. Sci. Lett. 157 (1998) 141–149.
[22] M. Jackson, Ö. Özdemir, Field and frequency dependence of a AC susceptibility in a natural single crystal of magnetite (abstract), EOS (Trans. Am. Geophys. Un.) 79 (Fall Meeting Suppl.) (1998) F237.
[23] M.E. Schabes, H.N. Bertram, Magnetization processes in ferromagnetic cubes, J. Appl. Phys. 64 (1988) 3882–3888.
[24] W. Williams, D.J. Dunlop, Three-dimensional micromagnetic modeling of ferromagnetic domain structure, Nature 337 (1989) 634–637.
[25] D.J. Dunlop, Ö. Özdemir, Rock Magnetism: Fundamentals and Frontiers, Cambridge University Press, New York, 1997, 573 pp.
[26] D.J. Dunlop, Temperature dependence of hysteresis in 0.04–0.22 μm magnetites and implications for domain structure, Phys. Earth Planet. Inter. 46 (1987) 100–119.
[27] D.J. Dunlop, Magnetite behavior near the single-domain threshold, Science 176 (1972) 41–43.
[28] D.J. Dunlop, The hunting of the 'psark', J. Geomagn. Geoelectr. 29 (1977) 293–318.
[29] Ö. Özdemir, S. Xu, D.J. Dunlop, Closure domains in magnetite, J. Geophys. Res. 100 (1995) 2193–2209.
[30] A.H. Morrish, L.A.K. Watt, Coercive force of iron oxide micropowders at low temperatures, J. Appl. Phys. 29 (1958) 1029–1033.

[31] E. Schmidbauer, N. Schembera, Magnetic hysteresis properties and anhysteresis remanent magnetization of spherical Fe_3O_4 particles in the grain size range 60–160 nm, Phys. Earth Planet. Inter. 46 (1987) 77–83.
[32] E. Schmidbauer, R. Keller, Magnetic properties and rotational hysteresis of Fe_3O_4 and γ-Fe_2O_3 particles $\sim$250 nm in diameter, J. Magn. Magn. Mater. 152 (1996) 99–108.
[33] K. Abe, Y. Miyamoto, S. Chikazumi, Magnetocrystalline anisotropy of low temperature phase of magnetite, J. Phys. Soc. Jpn. 41 (1976) 1894–1902.
[34] N. Tsuya, K.I. Arai, K. Ohmori, Effect of magnetoelastic coupling on the anisotropy of magnetite below the transition temperature, Physica 86–88B (1977) 959–960.
[35] J.P. Hodych, Evidence for magnetostrictive control of intrinsic susceptibility and coercive force of multidomain magnetite in rocks, Phys. Earth Planet. Inter. 42 (1986) 184–194.
[36] M. Ozima, M. Ozima, T. Nagata, Low temperature treatment as an effective means of 'magnetic cleaning' of natural remanent magnetization, J. Geomagn. Geoelectr. 16 (1964) 37–40.
[37] R.T. Merrill, Low-temperature treatments of magnetite and magnetite-bearing rocks, J. Geophys. Res. 75 (1970) 3343–3349.
[38] F. Heider, D.J. Dunlop, H. Soffel, Low-temperature and alternating field demagnetization of saturation remanence and thermoremanence in magnetite grains (0.037 μm to 5 mm), J. Geophys. Res. 97 (1992) 9371–9381.
[39] D.J. Dunlop, P.W. Schmidt, Ö. Özdemir, D.A. Clark, Paleomagnetism and paleothermometry of the Sydney Basin, 1. Thermoviscous and chemical overprinting of the Milton Monzonite, J. Geophys. Res. 102 (1997) 27271–27283.
[40] S. Chikazumi, K. Chiba, K. Suzuki, T. Yamada, Electron microscopic observation of low temperature phase of magnetite, in: Y. Hoshino, S. Iida, M. Sugimoto (Eds.), Ferrites: Proceedings of the International Conference, University of Tokyo Press, Tokyo, 1971, pp. 141–143.
[41] N. Otsuka, H. Sato, Observation of the Verwey transition in Fe_3O_4 by high-resolution electron microscopy, J. Solid State Chem. 61 (1986) 212–222.
[42] E.K.H. Salje, Phase Transitions in Ferroelastic and Co-Elastic Crystals, Cambridge University Press, Cambridge, 1993, 365 pp.
[43] S. Xu, R.T. Merrill, Microstress and coercivity in multidomain grains, J. Geophys. Res. 94 (1989) 10627–10636.
[44] B.M. Moskowitz, Micromagnetic study of the influence of crystal defects on coercivity in magnetite, J. Geophys. Res. 98 (1993) 18011–18026.